

## Kinetics and Mechanism of the Activation of Molecular Hydrogen by Bis(dimethylglyoximato)cobalt(II) Derivatives

By László I. Simándi,\* Éva Budó-Záhonyi, Zoltán Szeverényi, and Sándor Németh, Central Research Institute for Chemistry, Hungarian Academy of Sciences, 1525 Budapest, P.O. Box 17, Hungary

The reaction of  $H_2$  with bis(dimethylglyoximato)cobalt(II),  $[Co(Hdmg)_2]$ , and its 1 : 1 pyridine (py) adduct yields 3-aminobutan-2-one oxime *via* hydrogenation of the co-ordinated  $Hdmg^-$ . Excess of  $Hdmg^-$  is hydrogenated catalytically. The initial rate of  $H_2$  uptake is first order with respect to  $H_2$  pressure and second order with respect to overall cobalt concentration. Axial co-ordination of py,  $NEt_3H$ , and  $PPh_3$  enhances the rate, the five-co-ordinate adducts being more reactive than the parent cobaloxime(II). The spectrophotometric stability constants for the 1 : 1 and 1 : 2 py adducts are 186 and  $0.75\text{ dm}^3\text{ mol}^{-1}$ , respectively, at  $20^\circ\text{C}$ . The rate-determining step of  $H_2$  uptake is a bimolecular reaction of two hydridocobaloxime(III) species. In the absence of py, the overall rate coefficient is 3.1 and  $9.4\text{ dm}^6\text{ mol}^{-2}\text{ s}^{-1}$  in MeOH and 50% v/v methanol–water, respectively, at  $20^\circ\text{C}$ . For the reactions involving the 1 : 1 adduct with py, the corresponding values are 34.7 and  $323\text{ dm}^6\text{ mol}^{-2}\text{ s}^{-1}$ , respectively. Hydrogenation of the intermediate, containing one  $CH-NHOH$  moiety, is interpreted in terms of N–O bond cleavage by cobaloxime(II) followed by reduction of the resulting cobaloxime(III) by hydridocobaloxime(III).

SOLUTIONS of bis(dimethylglyoximato)cobalt(II),  $[Co(Hdmg)_2]$ , referred to as cobaloxime(II), as well as its mixed-ligand derivatives react with molecular hydrogen under ambient conditions<sup>1–4</sup> and in some cases the hydrogenation of certain unsaturated organic compounds has been noted.<sup>5–8</sup> In the presence of styrene<sup>3</sup> or hydroxide ions,<sup>4</sup> which are reactive scavengers for the hydridocobaloxime(III) formed in the system, 0.5 mol  $H_2$  per mol cobaloxime(II) is absorbed, producing  $[Co(Hdmg)_2(CHMePh)(py)]$  and cobaloxime(I), respectively. Under these conditions, the kinetics and mechanism of the reaction with  $H_2$  have been elucidated.<sup>3,4</sup> We now report on the behaviour of cobaloxime(II) systems containing no added scavenger.

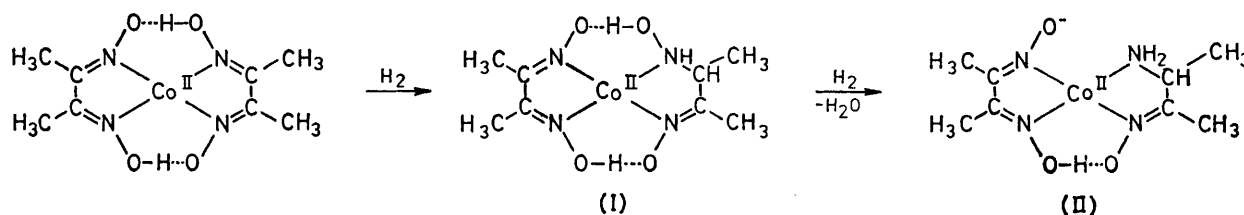
### RESULTS AND DISCUSSION

**Stoichiometry and Product.**—Solutions of  $[Co(Hdmg)_2]$  in methanol or 50% v/v methanol–water, prepared *in situ* by mixing  $Co[ClO_4]_2$ , dimethylglyoxime ( $H_2dmg$ ), and

results show that the amount of  $H_2$  absorbed in excess of the theoretical 0.5 mol  $H_2$  per mol cobaloxime(II) required for hydridocobaloxime(III) formation is due to hydrogenation of the co-ordinated dimethylglyoxime. Attempts to isolate the hydride or to detect reversibly absorbed  $H_2$  by freeze–thaw–pump cycles in the reacting solution have failed, indicating a very low level of hydride concentration.

The reaction was also followed by repetitive scanning of the u.v.–visible spectral region but at no time was it possible to detect even traces of cobaloxime(I), a conceivable alternative to hydridocobaloxime(III). The strong initial band in the 450–470 nm range decreases in intensity as  $H_2$  uptake progresses but no characteristic new bands appear.

Paper chromatograms obtained at various times during the reaction (samples exposed to air) reveal the slow accumulation and decay of an intermediate, as well as the presence of the reactant and one product. The three



SCHEME 1

$Na[OH]$  in a ratio of 1 : 2 : 2 under anaerobic conditions, absorb a total of 1.5–2.0 mol  $H_2$  per mol cobaloxime(II) over a period of 24 h. In the presence of added pyridine, the amount of absorption is somewhat higher (2.0–2.6 mol per mol). The addition of dimethylglyoxime in excess of the amount required for cobaloxime formation leads to the uptake of an extra 2.0 mol  $H_2$  per mol excess of  $H_2dmg$ . Upon exhaustive hydrogenation of a  $[Co(Hdmg)_2]-H_2dmg$  solution, 3-aminobutan-2-one oxime has been isolated and identified by gas chromatography (g.c.) as the predominant product. These

spots observed at various stages correspond to the air-oxidised derivatives of the cobalt(II) complexes involved.

These findings can be rationalised in terms of Scheme 1, in which (II) is a mixed-ligand derivative involving the hydrogenation product of dimethylglyoxime, 3-aminobutan-2-one oxime, as one of the equatorial ligands. The formation of (II) corresponds to the uptake of 2.0 mol  $H_2$  per mol cobaloxime(II). The structure proposed for the intermediate leading to the formation of (II) is represented by (I), in which one of the oxime groups is converted into a hydroxylamine moiety. This is not un-

reasonable in view of the obvious requirement that an intermediate characterised by a  $H_2$  uptake of 1.0 mol per mol cobaloxime(II) should exist.

*Effect of Axial Ligand on the Rate.*—The reactivities

TABLE 1

Effect of axial ligands (L) on the initial rate of  $H_2$  uptake ( $v_{in}$ ) at  $[Co]_T = 4 \times 10^{-3} \text{ mol dm}^{-3}$ ,  $[H_2]_{MeOH} = 3.3 \times 10^{-3} \text{ mol dm}^{-3}$ ,  $[H_2]_{MeOH/H_2O} = 9.95 \times 10^{-4} \text{ mol dm}^{-3}$ , and  $20^\circ \text{C}$

Solvent	Axial ligand	$10^3 [L]$ $\text{mol dm}^{-3}$	$10^7 v_{in}$ $\text{mol dm}^{-3} \text{ s}^{-1}$	$10^5 v_{in}/[H_2]$ $\text{s}^{-1}$
MeOH	py	0.0	1.7	5.15
		4.0	6.8	20.6
		16.0	13.6	41.2
		80.0	15.3	46.4
	PPh <sub>3</sub>	4.0	4.7	14.2
		16.0	5.0	15.1
	NEt <sub>2</sub> H	4.0	2.0	6.0
		8.0	1.8	5.5
	CN <sup>-</sup>	4.0	4.2	12.7
		16.0 *		
50% v/v Methanol-water	Br <sup>-</sup>	42.0	1.3	3.9
		42.0	1.2	3.6
	I <sup>-</sup>	42.0		
Methanol-water	H <sub>2</sub> O		1.5	15.1
	py	80.0	37.8	380

\* At this composition,  $[Co(CN)_5]^{3-}$  is formed and partly precipitated as the dimer.

toward  $H_2$  were characterised by the initial rates of hydrogen uptake ( $v_{in}$ ) measured volumetrically under vigorous stirring to ensure that the dissolution of  $H_2$

solvent, axial ligands with N, P, and C donor groups increase, whereas halides slightly decrease, the initial rate relative to the value measured without an added ligand. This effect is apparently due to the formation of 1:1 adducts whose reactivities differ from that of bis-(methanol)cobaloxime(II). The stability of the 1:1 adducts determines the ligand concentration at which a limiting rate, *i.e.* a plateau on the  $v_{in}$  vs.  $[L]$  curves, is observed. Assuming that in the ligand-concentration range corresponding to the plateau the five-co-ordinate 1:1 adduct is the major reacting species, the following reactivity order can be deduced from Table 1 for methanol as solvent:  $py > PPh_3 > CN^- > NEt_2H \approx MeOH > Br^- > I^-$ . Further increases in the ligand concentration should lead to at least partial formation of 1:2 adducts. The stability constants of the six-co-ordinate mixed-ligand complexes are, however, very small and/or the ligand solubility is limited, therefore extensive 1:2 adduct formation cannot be effected with the exception of py (see later). The bis(pyridine) adduct formed at *ca.*  $8 \text{ mol dm}^{-3}$  py was found to be unreactive towards  $H_2$ . Excess of cyanide converts the labile cobaloxime(II) derivative into  $[Co(CN)_5]^{3-}$ .

In 50% v/v aqueous methanol, both  $[Co(Hdmg)_2]$  and  $[Co(Hdmg)_2(py)]$  are more reactive than in pure MeOH (Table 1), consequently water as the sixth ligand is more favourable for the reaction than methanol. The relative reactivities of the complexes  $[Co(Hdmg)_2(py)L]$  therefore

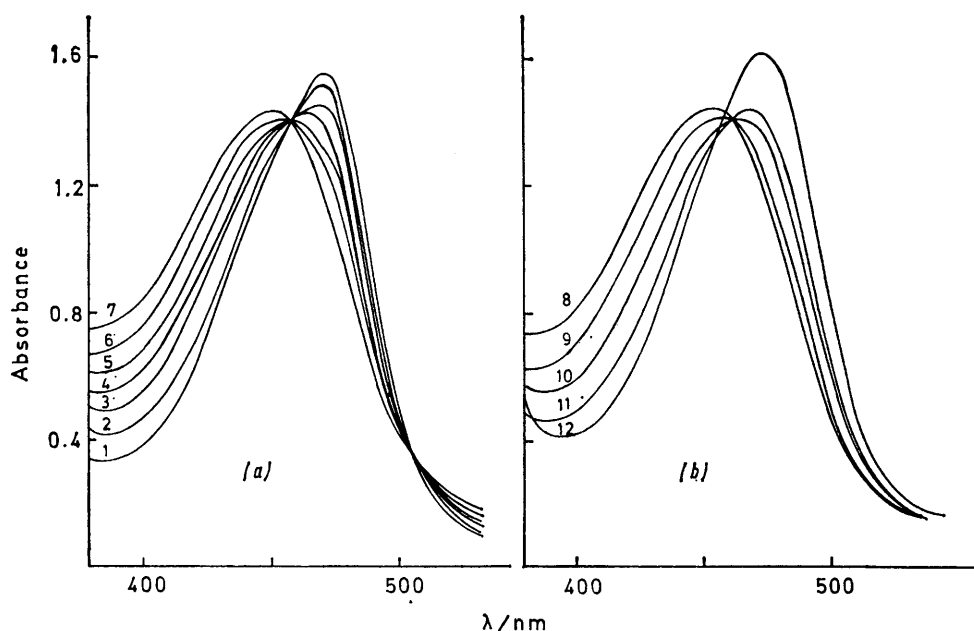


FIGURE 1 Spectra of cobaloxime(II) solutions in MeOH containing increasing amounts of pyridine: (a)  $[py]_T = 0.0-0.08 \text{ mol dm}^{-3}$ ; (b)  $[py]_T = 0.30-11 \text{ mol dm}^{-3}$ ;  $[Co]_T = 4 \times 10^{-3} \text{ mol dm}^{-3}$ ;  $20^\circ \text{C}$ ; 0.1 cm cells.  $[py]_T/\text{mol dm}^{-3} = 0$  (1),  $2 \times 10^{-3}$  (2),  $4 \times 10^{-3}$  (3),  $6 \times 10^{-3}$  (4),  $10 \times 10^{-3}$  (5),  $16 \times 10^{-3}$  (6),  $64 \times 10^{-3}$  (7), 0.29 (8), 0.58 (9), 1.16 (10), 2.32 (11), and 11.0 (12)

was not rate-determining (*cf.* Experimental section). At constant concentration of  $[Co(Hdmg)_2]$ , the initial rate depends markedly on the nature and concentration of unidentate ligands forming 1:1 (and possibly 1:2) mixed-ligand complexes *via* axial co-ordination. The relevant data are shown in Table 1. In methanol as

decrease in the following order with respect to L:  $H_2O > MeOH \gg py$ .

*Stability of Pyridine Adducts.*—Since the detailed kinetic studies were carried out with py as axial ligand, the relevant stepwise stability constants were determined by a spectrophotometric technique under anaero-

bic conditions. The spectral changes observed upon increasing the pyridine concentration in a  $4 \times 10^{-3}$  mol  $\text{dm}^{-3}$  cobaloxime(II) solution from zero to 11.0 mol  $\text{dm}^{-3}$  are shown in Figure 1(a) and (b). The two isosbestic points at 455 and 505 nm [Figure 1(a)] are consistent with a single equilibrium corresponding to equations (1) and (3), where  $\text{Co}'$  indicates  $\text{Co}(\text{Hdmg})_2$ . At higher py concentrations, the spectral changes are reversed and the isosbestic points become less distinct, indicating the additional presence of the 1 : 2 adduct, *cf.* equations (2)

yield  $1/K_1$  and  $\epsilon_{\text{Co}'(\text{py})}$ , respectively. A similar plot based on equation (6) can be used to determine  $K_2$  and  $\epsilon_{\text{Co}'(\text{py})_2}$ . The results are summarised in Table 2.

The stability constants are in fair agreement with earlier data based on e.s.r. spectroscopy.<sup>9</sup> The observed spectra indicate no displacement of the equatorial  $\text{Hdmg}^-$  ligands by py even at 11.0 mol  $\text{dm}^{-3}$  pyridine. This is in full agreement with the high thermodynamic stability of the hydrogen-bonded  $\text{Co}(\text{Hdmg})_2$  chelate system as opposed to the low stability of  $\text{Co}^{\text{II}}\text{-py}$  com-

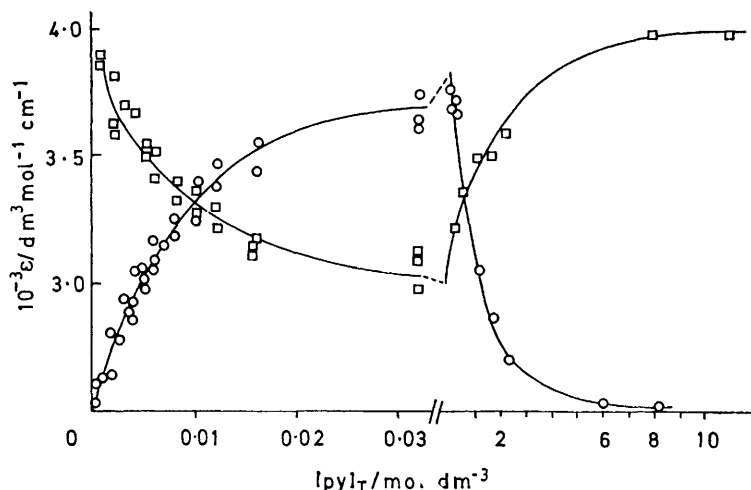
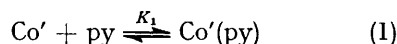


FIGURE 2 Dependence of  $\epsilon$  ( $= A/l[\text{Co}]_T$ ) on  $[\text{py}]_T$  at 420 ( $\square$ ) and 470 nm ( $\circ$ )

and (4). Equilibria (1) and (2) do not overlap significantly as demonstrated by the curves in Figure 2,



$$K_1 = [\text{Co}'(\text{py})]/[\text{Co}'][\text{py}] \quad (3)$$

$$K_2 = [\text{Co}'(\text{py})_2]/[\text{Co}'(\text{py})][\text{py}] \quad (4)$$

where  $\epsilon$  ( $= A/l[\text{Co}]_T$ ) is plotted against the total concentration of pyridine for 420 and 470 nm. Consequently,  $K_1$  and  $K_2$  can be determined by a simple graphical procedure based on equations (5) and (6),

$$\epsilon = \epsilon_{\text{Co}'(\text{py})} + \frac{1}{K_1} (\epsilon_{\text{Co}'} - \epsilon) \frac{1}{[\text{py}]} \quad (5)$$

$$\epsilon = \epsilon_{\text{Co}'(\text{py})_2} + \frac{1}{K_2} (\epsilon_{\text{Co}'(\text{py})} - \epsilon) \frac{1}{[\text{py}]} \quad (6)$$

derived on the assumption that (1) and (2) are separate equilibria, each involving two absorbing species. The concentrations of free pyridine,  $[\text{py}]$ , were calculated using  $K_1 = 200 \text{ dm}^3 \text{ mol}^{-1}$  obtained from the half-height of the  $\epsilon$  vs.  $[\text{py}]_T$  curve at low pyridine concentrations. In principle, this is an iteration procedure, which, however, converges after the first step. At higher pyridine concentrations, the assumption  $[\text{py}] \approx [\text{py}]_T$  is perfectly acceptable. If  $\epsilon$  is plotted against  $(\epsilon_{\text{Co}'} - \epsilon)/[\text{py}]$ , the slope and intercept of the straight line obtained

plexes, and with the e.s.r. spectra of the  $[\text{Co}(\text{Hdmg})_2]\text{-py}$  system.<sup>9</sup> Mixed-ligand complex formation in similar chelate systems is thus mostly restricted to the axial position(s). A known exception is cyanide ion, which, however, is a very good ligand for  $\text{Co}^{\text{II}}$ , as evidenced by

TABLE 2

Stepwise stability constants and molar absorption coefficients for the complexes in equilibria (1) and (2)

$\lambda$ nm	$K_1$ $\text{dm}^3 \text{ mol}^{-1}$	$K_2$	$\epsilon_{\text{Co}'}$ $\text{dm}^3 \text{ mol}^{-1} \text{ cm}^{-1}$	$\epsilon_{\text{Co}'(\text{py})}$ $\text{dm}^3 \text{ mol}^{-1} \text{ cm}^{-1}$	$\epsilon_{\text{Co}'(\text{py})_2}$ $\text{dm}^3 \text{ mol}^{-1} \text{ cm}^{-1}$
420	186	0.73	1 450	2 950	1 140
470	185	0.78	3 900	2 800	4 150

the high stability of  $[\text{Co}(\text{CN})_5]^{3-}$  (*cf.* footnote to Table 1).

**Kinetics of  $\text{H}_2$  Uptake.**—As illustrated by Figure 3(a)–(d), the initial rate of  $\text{H}_2$  uptake is proportional to  $[\text{Co}]_T^2$  both in the presence and absence of pyridine, and

$$v_{\text{in}} = k_{\text{obs}}[\text{Co}]_T^2[\text{H}_2] \quad (7)$$

to the partial pressure of  $\text{H}_2$ . Consequently, the rate law is of the form (7), where  $[\text{Co}]_T$  is the initial overall cobaloxime(II) concentration, as defined by equation (8).

$$[\text{Co}]_T = [\text{Co}'] + [\text{Co}'(\text{py})] + [\text{Co}'(\text{py})_2] \quad (8)$$

The effect of py concentration on  $v_{\text{in}}$  is illustrated by the curves in Figure 4. In the concentration range studied, py increases the reactivity towards  $\text{H}_2$  up to a limiting value, which is due to the gradual shift of equilibrium (1) to the right,  $\text{Co}'(\text{py})$  being more reactive

than  $\text{Co}'$ . The second-order dependence on  $[\text{Co}]_{\text{T}}$  implies that two molecules of cobaloxime(II) are required to activate one molecule of  $\text{H}_2$ . Clearly, at  $[\text{py}] = 0$  only  $\text{Co}'$  is present. However, if py is also present, two more

(4), (8), and (9) leads to expression (10) for  $v_{\text{in}}$ , where  $x = [\text{Co}']/[\text{Co}]_{\text{T}}$  and  $y = [\text{Co}'(\text{py})]/[\text{Co}]_{\text{T}}$ . Comparison of equations (7) and (10) gives  $k_{\text{obs}}$  in terms of the three individual rate constants. Since  $k_{\text{Co}'}$  is known from

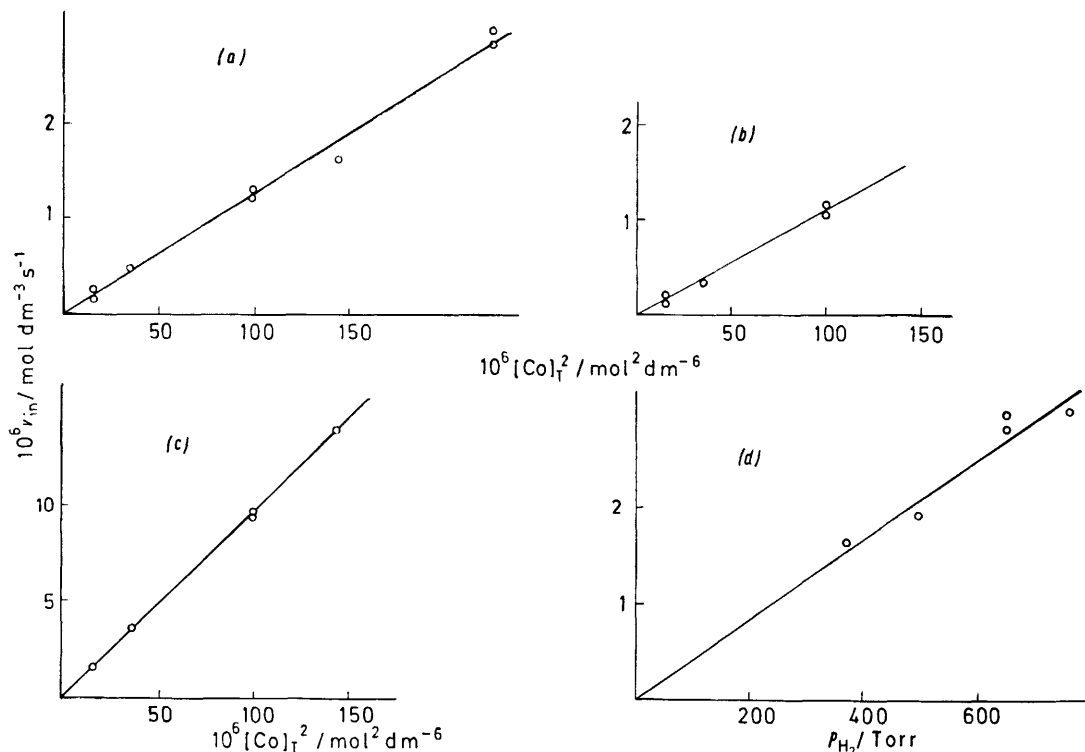


FIGURE 3 Dependence of the initial rate of  $\text{H}_2$  uptake ( $v_{\text{in}}$ ) on  $[\text{Co}]_{\text{T}}^2$  and on the  $\text{H}_2$  concentration (partial pressure). (a)  $[\text{py}]_{\text{T}} = 0.0$ , solvent MeOH; (b)  $[\text{py}]_{\text{T}} = 0.0$ , solvent 50% v/v methanol-water; (c)  $[\text{py}]_{\text{T}} = 0.08 \text{ mol dm}^{-3}$ , solvent MeOH; (d)  $[\text{py}]_{\text{T}} = 0.0$ ,  $[\text{Co}]_{\text{T}} = 15 \times 10^{-3} \text{ mol dm}^{-3}$ , solvent MeOH

possibilities arise, involving the pairs  $\text{Co}'$ ,  $\text{Co}'(\text{py})$  and  $\text{Co}'(\text{py})$ ,  $\text{Co}'(\text{py})$ . Consequently, rate law (7) should be the sum of three terms as in equation (9), where  $[\text{Co}']$

runs with  $[\text{py}] = 0$ , the validity of equation (10) can be demonstrated by rearranging it to (11) and plotting the left-hand side against  $x/y$ . Using the experimental points shown in Figure 4, one obtains the straight lines

$$v_{\text{in}} = \{k_{\text{Co}'}[\text{Co}']^2 + k_{\text{Co}'(\text{py})}[\text{Co}'(\text{py})]^2 + k_{\text{Co}',\text{Co}'(\text{py})}[\text{Co}'][\text{Co}'(\text{py})]\}[\text{H}_2] \quad (9)$$

$$v_{\text{in}} = (k_{\text{Co}'}x^2 + k_{\text{Co}'(\text{py})}y^2 + k_{\text{Co}',\text{Co}'(\text{py})}xy)[\text{Co}]_{\text{T}}^2[\text{H}_2] \quad (10)$$

$$\frac{1}{y^2} \left( \frac{v_{\text{in}}}{[\text{Co}]_{\text{T}}^2[\text{H}_2]} - k_{\text{Co}'}x^2 \right) = k_{\text{Co}'(\text{py})} + k_{\text{Co}',\text{Co}'(\text{py})}(x/y) \quad (11)$$

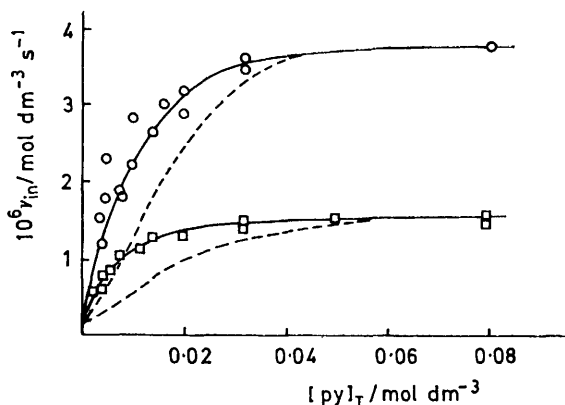


FIGURE 4 Dependence of the initial rate of  $\text{H}_2$  uptake on the pyridine concentration, at 20 °C in MeOH ( $\square$ ) and 50% v/v methanol-water ( $\circ$ ) as solvent. The solid lines are experimental curves, the broken lines are calculated for the 'symmetrical' routes only

and  $[\text{Co}'(\text{py})]$  are the concentrations of the individual species. In this treatment,  $\text{Co}'(\text{py})_2$  is disregarded as a reactant but its concentration is taken into account in balancing the equations. Combination of equations (3),

displayed in Figure 5. The rate constants determined from the slope and intercept are listed in Table 3 for both MeOH and 50% v/v MeOH-water. The importance of the third term in equation (10), *i.e.* the contribution of a reaction path involving a  $\text{Co}'$  and a  $\text{Co}'(\text{py})$  complex, is demonstrated by the broken lines in Figure 4, which were calculated on the assumption that only the two 'symmetrical' routes exist. In these calculations  $k_{\text{Co}'}$  was the same as in Table 3 but  $k_{\text{Co}'(\text{py})}$  was deduced from the limiting rates of Figure 4 and the stepwise stability constants. Clearly, the broken line deviates from the experimental points. The solid line, however, which was calculated using the three resolved rate

constants listed in Table 3, gives a fairly good fit, lending support to the three-term rate law (9).

The activation parameters have been determined under conditions where the  $k_{\text{Co}'(\text{py})}$  term predominates (Table 4). Consequently, the values of  $\Delta H^\ddagger = 54 \text{ kJ}$

TABLE 3

Rate coefficients ( $\text{dm}^6 \text{ mol}^{-2} \text{ s}^{-1}$ ) for the cobaloxime(II)- $\text{H}_2$  reaction at  $20^\circ \text{C}$

Solvent	$k_{\text{Co}'}$	$k_{\text{Co}'(\text{py})}$	$k_{\text{Co}',\text{Co}'(\text{py})}$
MeOH	3.1	34.7	32.2
50% v/v Methanol-water	9.4	323	365

$\text{mol}^{-1}$  and  $\Delta S^\ddagger = -33 \text{ J K}^{-1} \text{ mol}^{-1}$  obtained from the Arrhenius plot of the data in Table 4 refer to the route involving two  $\text{Co}'(\text{py})$  molecules.

**Mechanism.**—In the absence of pyridine, the observed

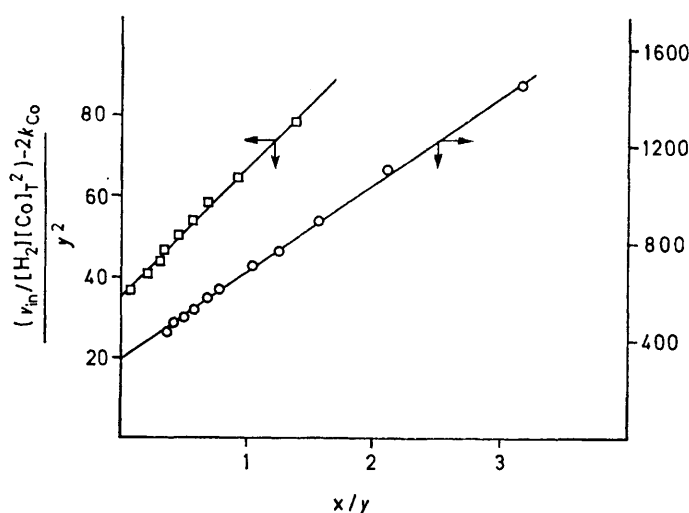


FIGURE 5 Plot of the data in Figure 4 according to equation (11). Solvents and temperatures as in Figure 4

kinetic behaviour is consistent with the mechanism depicted by equations (12)–(14) where (I) is the intermediate in Scheme 1. Added pyridine converts part of the  $\text{Co}'$  species into the more reactive five-co-ordinate  $\text{Co}'(\text{py})$ . An analogous mechanism, written for  $\text{Co}'(\text{py})$ ,

TABLE 4

Temperature dependence of the rate of  $\text{H}_2$  uptake at  $[\text{Co}]_T = 4 \times 10^{-3} \text{ mol dm}^{-3}$ ,  $[\text{py}]_T = 0.1 \text{ mol dm}^{-3}$ , and with MeOH as solvent

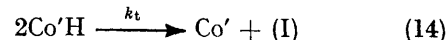
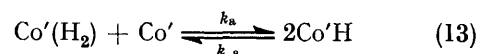
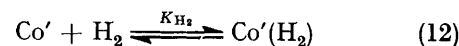
$T$ K	$10^6 v_{\text{in}}$ $\text{mol dm}^{-3} \text{ s}^{-1}$	$10^3 [\text{H}_2]$ $\text{mol dm}^{-3}$	$K_1$ $\text{dm}^3 \text{ mol}^{-1}$	$K_2$ $\text{mol}^{-1}$	$\gamma$	$k_{\text{Co}'(\text{py})}$ $\text{dm}^6 \text{ mol}^{-2} \text{ s}^{-1}$
293	1.50	3.33	175	0.83	0.877	36.6
303	2.80	3.00	152*	0.70*	0.881	75.3
313	5.70	3.07	131	0.58	0.885	148

\* Calculated value.

is operative on the plateau in Figure 4. Before the plateau, however, non-symmetrical reactions involving  $\text{Co}'$  and  $\text{Co}'(\text{py})$  do certainly take place, *cf.* the third term in rate law (9). The mechanisms including 'cross' reactions of this type can be derived by replacing  $\text{Co}'$  by  $\text{Co}'(\text{py})$ ,  $\text{Co}'\text{H}$  by  $\text{Co}'\text{H}(\text{py})$ , *etc.*, to produce a maximum of three additional routes. The complexity of the

corresponding rate equations precludes a detailed treatment that would yield an expression of the rate coefficient  $k_{\text{Co}',\text{Co}'(\text{py})}$ , *cf.* equation (9), in terms of individual rate constants of the possible non-symmetrical steps.

Mechanism (12)–(14) and its counterpart for  $\text{Co}'(\text{py})$  accounts for the kinetic behaviour as deduced from the initial rates, when product (II) is not yet present in



significant amounts. This requires that steps (12) and (13) be regarded as pre-equilibria and (14) as rate-determining. In the absence of py,  $k_{\text{obs}}$  can be expressed as in equation (15), where  $K_a = k_a/k_{-a}$ . On the plateau

$$k_{\text{obs}} = k_{\text{Co}'} = K_{\text{H}_2} K_a k_t \quad (15)$$

of the  $v_{\text{in}}$  vs.  $[\text{py}]$  curve, both the  $k_{\text{Co}'}$  path and the 'cross' routes are negligible, therefore, equation (16) is valid. (The superscript py refers to constants in the presence of pyridine.) The factor in parentheses takes into

$$k_{\text{obs,py}} = K_{\text{H}_2}^{\text{py}} K_a^{\text{py}} k_t^{\text{py}} \left( \frac{K_1 [\text{py}]_T}{1 + K_1 [\text{py}]_T + K_1 K_2 [\text{py}]_T^2} \right)^2 \quad (16)$$

account the effect of equilibria (1) and (2) on the actual  $\text{Co}'(\text{py})$  concentration, assuming that  $[\text{py}] \approx [\text{py}]_T$ . In the two limiting cases discussed, the concentration of  $\text{Co}'\text{H}$  and  $\text{Co}'\text{H}(\text{py})$  can be expressed by equations (17) and (18). Clearly, if the rate is now written as in

$$[\text{Co}'\text{H}] = [\text{Co}'](K_{\text{H}_2} K_a [\text{H}_2])^\ddagger \quad (17)$$

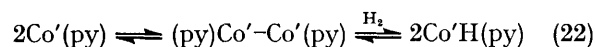
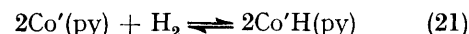
$$[\text{Co}'\text{H}(\text{py})] = [\text{Co}'(\text{py})](K_{\text{H}_2}^{\text{py}} K_a^{\text{py}} [\text{H}_2])^\ddagger \quad (18)$$

$$v_{\text{in}} = k_t [\text{Co}'\text{H}]^2 \quad (19)$$

equation (19), the empirical rate law for  $[\text{py}] = 0$  is readily obtained using equations (15) and (17). Similarly, the kinetic equation for the ' $\text{Co}'(\text{py})$  only' path can be produced by combining equation (20) with (16) and (18).

$$v_{\text{in,py}} = k_t^{\text{py}} [\text{Co}'\text{H}(\text{py})]^2 \quad (20)$$

Steps (12) and (13) represent the homolytic formation of hydridocobaloxime(III). Two other mechanistic alternatives are conceivable, *viz.* a termolecular step,



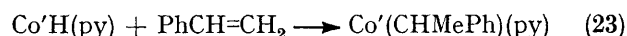
equation (21), and dimerisation followed by reaction with  $\text{H}_2$ , equation (22), but objections can be raised to both of these possibilities. The probability of termolecular collisions is generally very low compared with bimolecular steps. Dimerisation would remove the likely centre of reactivity, *viz.* the unpaired cobalt  $d$



electron, and impose considerable steric hindrance to the approach of  $H_2$ ; also e.s.r. studies in MeOH provide no evidence for dimerisation,<sup>9</sup> which is only observed in non-co-ordinating solvents. No straightforward bonding picture can be proposed for the  $Co'(H_2)$  species, which is why Martell and Taqui Khan<sup>10</sup> were critical of this formulation given for  $[Co(CN)_5]^{3-}$ . We regard  $Co'(H_2)$  and  $Co'(H_2)(py)$  as short-lived 'collision complexes' existing as a result of unspecified weak interactions, their lifetimes being sufficient to eliminate the necessity of ternary collisions. Also, the bimolecular, homolytic mechanism of the decomposition of  $[Co(CN)_5H]^{3-}$ <sup>11</sup> and that of  $[CoH(Hdmg)_2(PBu_3)]$ <sup>12</sup> can be best pictured as involving the  $Co \cdots H \cdots H \cdots Co$  moiety in the transition state, and microscopic reversibility requires the same activated complex for their formation. This

the py concentration and the rate equation contains a first-order term in  $[Co]_T$ . The reason for this discrepancy is not clear at the moment.

Previous work has shown that excess of styrene<sup>3</sup> or  $Na[OH]$ <sup>4</sup> strongly increases the initial rate of  $H_2$  uptake in MeOH. When present in sufficient concentration, styrene reacts rapidly with  $Co'H(py)$  to give the stable organocobalt complex  $Co'(CHMePh)(py)$ , equation (23), shifting the rate-determining step to  $Co'H(py)$  formation, equation (13). Similarly,  $Na[OH]$  deprotonates  $Co'H(py)$  in a fast step, equation (24), resulting in the



formation of pyridinecobaloxime(i), again with step (13) rate-determining. These two scavengers yield rate coefficients  $K_{H_2}^{py}k_a^{py}$  in fair agreement with each other, confirming the identity of the rate-determining step. Since the limiting rates observed with the scavengers are much higher than the rates of  $H_2$  uptake by  $Co'$  or  $Co'(py)$ , studied in this work, we conclude that in MeOH step (14) is rate-determining, with (12) and (13) as pre-equilibria. The failure to detect  $Co'H$  or  $Co'H(py)$  implies that these species reach only very low equilibrium concentrations. Additional support for this view is obtained by dividing  $K_{H_2}k_a$  and  $K_{H_2}^{py}k_a^{py}$ , the rate coefficients in the presence of added styrene,<sup>3</sup> by  $K_{H_2}K_a k_t$  and  $K_{H_2}^{py}K_a^{py}k_t^{py}$ , respectively (this work), which yield  $k_{-a}/k_t = 2.35$  and  $k_{-a}^{py}/k_t^{py} = 43.3$ . We can give no estimate for  $K_{H_2}K_a$  and  $K_{H_2}^{py}K_a^{py}$ , the overall equilibrium constants for hydridocobaloxime(iii) formation using the data of this work. However, computer simulation of the behaviour of the autocatalytic cobaloxime(ii)-cobaloxime(iii)-hydrogen system<sup>13</sup> yielded a value of  $K_{H_2}^{py}K_2^{py} = 4 \times 10^{-4} \text{ dm}^3 \text{ mol}^{-1}$ . Thus  $[CoH(Hdmg)_2(py)]$  is much less stable than  $[CoH(Hdmg)_2(PBu_3)]$ , for which Chao and Espenson<sup>12</sup> have estimated a formation equilibrium constant of  $0.18 \text{ dm}^3 \text{ mol}^{-1}$ .

The participation of two hydridocobaloxime(iii) molecules in rate-determining step (14) is supported by the first-order dependence of  $v_{in}$  on the  $H_2$  pressure. A  $Co' + Co'H$  combination implies a half-order dependence on the pressure of  $H_2$ , which is inconsistent with the observed rate law.

The higher reactivity of  $Co'(py)$  as compared with  $Co'$  seems to be due to the more extensive delocalisation of the unpaired  $d$  electron along the  $z$  axis, as shown by earlier e.s.r. measurements.<sup>9,14</sup> Such delocalisation enhances the free-radical character of cobaloxime(ii), thus facilitating formal H-atom abstraction (homolytic cleavage) from the  $H_2$  molecule. Similar factors are operative with the other axial ligands too. Apparently, the acceleration is a cumulative effect and no individual rate or equilibrium constant can be singled out as responsible for the overall increase in reactivity. Previous work<sup>3</sup> has yielded  $K_{H_2}^{py}k_a^{py}/K_{H_2}k_a = 205$ , and the data in this paper give  $K_{H_2}^{py}k_a^{py}k_t^{py}/K_{H_2}K_a k_t = 11.2$ . This indicates that the  $H_2$ -activation steps, *i.e.* (12) and

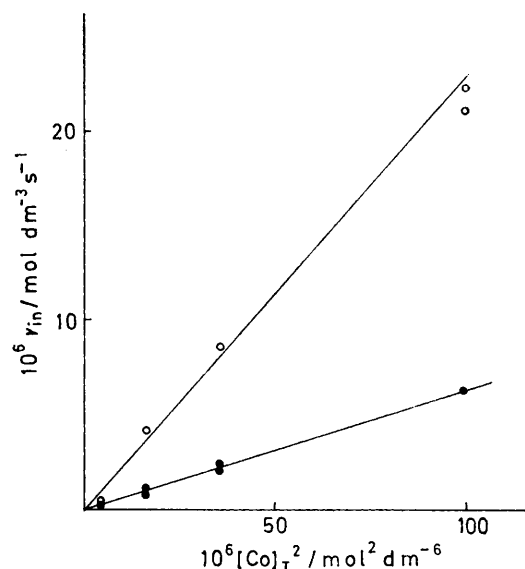


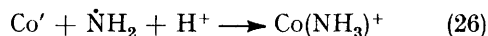
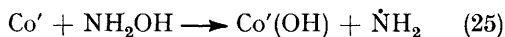
FIGURE 6 Dependence of the initial rate of  $H_2$  uptake ( $v_{in}$ ) on  $[Co]_T^2$  in the absence (●) and presence (○) of excess of  $Na[OH]$  ( $[OH]_{excess} = [Co]_T$ ). Solvent MeOH, 20 °C

again favours steps (12) and (13) as opposed to (21) or (22).

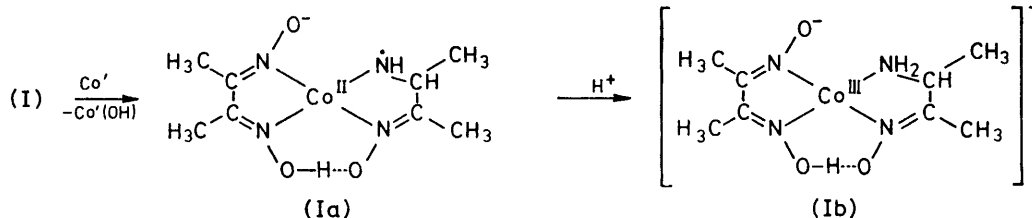
**Effect of Excess of  $Na[OH]$ .**—The rate of  $H_2$  absorption is increased by  $Na[OH]$  added in excess of the amount required for cobaloxime(ii) formation. However, under such conditions some or all of the cobaloxime(ii) ends up as cobaloxime(i), recognised by its strong absorption in the 500–700 nm range. The last species arises from rapid deprotonation of the hydridocobaloxime(iii), which makes hydride formation rate-determining.<sup>4</sup> Thus the observed increase in rate can be explained by the scavenging effect of  $Na[OH]$  [see equation (24)], rather than by a new route, *e.g.* heterolytic cleavage of  $H_2$ . This receives support from the fact that the kinetic order with respect to  $[Co]_T$  remains 2 in the presence of excess of  $Na[OH]$ , with no first-order dependence on  $[Co]_T$  in the rate equation (Figure 6). This is at variance with the results of Yamaguchi and Miyagawa,<sup>8</sup> who report that the order with respect to  $[Co]_T$  varies with

(13), are accelerated by added py to a greater extent than is transfer step (13).

The transformation of intermediate (I) into product (II) (*cf.* Scheme 1) can be rationalised by analogy with the known formal oxidative addition of hydroxylamine to cobaloxime(II), yielding hydroxo- and ammine-cobaloxime(III), as in equations (25) and (26).<sup>15</sup> A

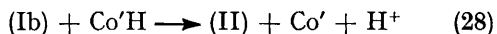
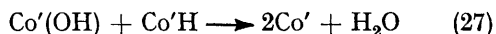


similar reaction involving N-O bond cleavage at the substituted hydroxylamine moiety in intermediate (I)



SCHEME 2

is in Scheme 2. We have previously observed that cobaloxime(III) derivatives can be reduced to cobaloxime(II) complexes in the presence of cobaloxime(II) and molecular  $\text{H}_2$ ,<sup>13</sup> the reactive species being hydrido-cobaloxime(III), *i.e.*  $\text{Co}'\text{H}$  or  $\text{Co}'\text{H}(\text{py})$ . In the systems studied in this work, the products of the reactions in Scheme 2, *i.e.*  $\text{Co}'(\text{OH})$  and (Ib), respectively, can be similarly reduced by the hydrido-species formed *via* steps (12) and (13) or the corresponding  $\text{Co}'(\text{py})$  route, as in equations (27) and (28). This implies that no



species other than the original cobaloxime(II) derivatives are reactive towards  $\text{H}_2$  and the observed products can be readily accounted for by combining previously known reactions.

**Catalytic Hydrogenation of Dimethylglyoxime.**—Although cobaloxime(II) complexes have been known for some time<sup>16</sup> to react with molecular hydrogen, their use as homogeneous catalysts in the hydrogenation of olefinic and other substrates is still rather restricted. This is apparently due to at least two reasons: (*i*) the ligand-hydrogenation process described in this paper inherently competes with the hydrogenation (reduction) of any added substrate; (*ii*) with many olefins, *e.g.* styrene, reactive hydridocobaloximes readily form stable organo-cobalt derivatives that are not hydrogenated. A catalytic hydrogenation (reduction) process may occur *via* H-atom transfer or electron transfer to suitable reactive acceptors such as cobaloxime(III)<sup>13</sup> or nitro- or diene compounds, but the reduction product should be unreactive towards the cobaloxime(II) catalyst, or should react with it reversibly. We have found that

cyclohexa-1,3-diene can be hydrogenated to cyclohexene in *ca.* 72% yield. In this case, the formation of a cyclohexenylcobaloxime derivative is sterically hindered but the diene is a good H-atom acceptor, and the intermediate free-radical abstracts a second H atom from hydridocobaloxime. The only case when these complications do not arise is the catalytic hydrogenation of free dimethylglyoxime added in excess of the amount required for cobaloxime(II) formation. Figure 7 shows the volumetric  $\text{H}_2$  absorption curves for a  $4 \times 10^{-3} \text{ mol dm}^{-3}$  pyridinecobaloxime(II) solution (*a*), and for the same solution containing additional  $16 \times 10^{-3} \text{ mol dm}^{-3}$  free dimethylglyoxime (*b*). In the latter case, the rate

of  $\text{H}_2$  uptake remains unchanged for a long period of time, its magnitude being equal to  $v_m$  determined from curve (*a*). According to Table 5, the initial rate is independent of the dimethylglyoxime concentration but is second order overall in cobaloxime(II) concentration.

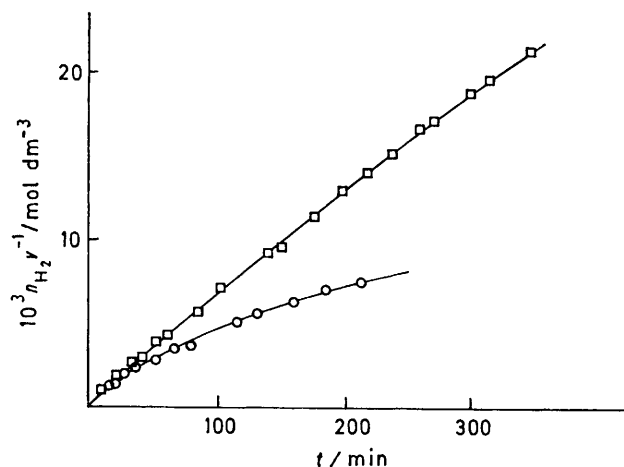


FIGURE 7  $\text{H}_2$  absorption curves for pyridinecobaloxime(II) recorded in the absence (O) and presence (□) of excess of dimethylglyoxime ( $16 \times 10^{-3} \text{ mol dm}^{-3}$ ).  $[\text{Co}]_T = 4 \times 10^{-3} \text{ mol dm}^{-3}$ ,  $[\text{py}]_T = 80 \times 10^{-3} \text{ mol dm}^{-3}$ , buffer =  $0.05 \text{ mol dm}^{-3}$  borax and  $0.08 \text{ mol dm}^{-3} \text{HClO}_4$ ,  $20^\circ \text{C}$

The exhaustive hydrogenation of  $0.1 \text{ mol dm}^{-3} \text{H}_2\text{dmg}$  in the presence of  $8 \times 10^{-3} \text{ mol dm}^{-3} [\text{Co}(\text{Hdmg})_2]$  for 10 d afforded 3-aminobutan-2-one oxime in 94% yield. The product was identified and estimated by comparing the gas chromatograms of the solution on three different columns with those of authentic 3-aminobutan-2-one oxime, prepared by a known procedure.<sup>17</sup> The tetramethylpyrazine detected<sup>1</sup> upon the hydrogenation of

cobaloximes by Pt/C was probably formed *via* hydrolysis, condensation and oxidation of 3-aminobutan-2-one oxime, the primary hydrogenation product.

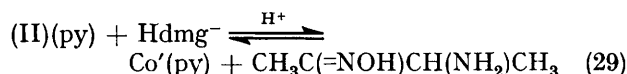
These results clearly show that the catalytic hydrogenation of free dimethylglyoxime occurs by the same route as that of co-ordinated Hdmg<sup>−</sup>, *viz. via* steps (12)—(14) and Scheme 2. The 2-aminobutan-2-one oxime

TABLE 5

Initial rates of H<sub>2</sub> uptake at various concentrations of excess of dimethylglyoxime and [py]<sub>T</sub> = 0.08 mol dm<sup>−3</sup>, buffer 0.05 mol dm<sup>−3</sup> borax and 0.08 mol dm<sup>−3</sup> HClO<sub>4</sub>, 50% v/v methanol–water as solvent, and 20 °C

$10^3[\text{Co}]_{\text{T}}$ mol dm <sup>−3</sup>	$10^3[\text{H}_2\text{dmg}]_{\text{excess}}$ mol dm <sup>−3</sup>	$10^6v_{\text{in}}$ mol dm <sup>−3</sup> s <sup>−1</sup>
4.0	0.0	0.98
4.0	8.0	1.01
4.0	16.0	1.02
2.0	0.0	0.27
2.0	4.0	0.25
2.0	8.0	0.28
2.0	16.0	0.24

ligand in (II) is, however, continuously exchanged with free Hdmg<sup>−</sup> according to equation (29). For cobalt(II),



being a labile metal ion, this ligand exchange is apparently rather fast, and the excess of Hdmg<sup>−</sup> shifts the equilibrium to the right.

#### EXPERIMENTAL

The rate of hydrogen absorption was measured volumetrically at constant pressure. The gas burette permitted readings with an accuracy of 0.05 cm<sup>3</sup>; the overall H<sub>2</sub> uptakes amounted to 40–60 cm<sup>3</sup>. In a typical run for rate measurements, the H<sub>2</sub> uptake was followed for *ca.* 60 min (absorbed H<sub>2</sub> 15–30 cm<sup>3</sup>). The initial slope of the uptake curve was determined from 4–6 points read at 1–2 min intervals; the points were found to define a straight line in most cases, curvatures being subsequently observed. The reproducibility of initial slopes was of the order of ±5%. The H<sub>2</sub> absorption rates were calculated from the initial slope (cm<sup>3</sup> H<sub>2</sub> absorbed per dm<sup>3</sup> solution per second) using equation (30) where *C* converts the absorbed volume

$$v \text{ mol dm}^{-3} \text{ s}^{-1} = C \cdot \text{slope} \quad (30)$$

to mol H<sub>2</sub>, taking into account the temperature (20 °C) and the partial pressure of H<sub>2</sub> during the measurement.

The rates of H<sub>2</sub> uptake were measured under vigorous stirring and were unaffected by further increases in the stirring speed (no diffusion control). The concentration of H<sub>2</sub> was assumed to be equal to the saturation value in the given solvent. The solubility of H<sub>2</sub> was determined for both MeOH and 50% v/v methanol–water by removing dissolved H<sub>2</sub> from a saturated solution by repeated freeze-thaw–pump cycles, then collecting it in a calibrated vessel. The solubilities obtained are 0.091 0 ± 0.000 5 and 0.023 6 ± 0.000 5 cm<sup>3</sup> H<sub>2</sub> per cm<sup>3</sup> solvent for MeOH and 50% v/v

methanol–water, respectively (20 °C; H<sub>2</sub> pressure 760 Torr).\*

The cobaloxime(II) solutions were prepared by mixing Co[ClO<sub>4</sub>]<sub>2</sub>·6H<sub>2</sub>O, dimethylglyoxime, and Na[OH] in a ratio of 1:2:2 under strictly anaerobic conditions. The cobalt perchlorate solution was deaerated and saturated with H<sub>2</sub> in a separate compartment. After thermal equilibration, it was mixed with a deaerated and H<sub>2</sub>-saturated solution containing all the other components. When necessary, the cobaloxime(II) solution could be transferred into a spectrophotometric cell and sealed with the exclusion of air. Reagent-grade chemicals were used throughout.

The u.v.–visible spectra were recorded on a Beckman ACTA MIV instrument. The paper chromatograms were run on Whatman 1 paper, using 2 mol dm<sup>−3</sup> aqueous propanol–aqueous pyridine (70:30) for elution, after exposing the sample to air.

The product 3-aminobutan-2-one oxime was isolated as the hydrochloride after acidification with HCl, followed by evaporation to dryness and separation from the inorganic material, m.p. 157–161 °C (lit.<sup>17</sup> 160–162 °C) (Found: C, 35.0; H, 8.75; Cl, 24.4; N, 19.7. Calc. for C<sub>4</sub>H<sub>11</sub>ClN<sub>2</sub>O: C, 34.6; H, 8.00; Cl, 25.6; N, 20.2%). The yield of the oxime in the hydrogenation of excess of dimethylglyoxime was determined by comparing the gas chromatograms of the product solution with those of authentic material<sup>17</sup> on 3% E-301, 3% OV-17, and GE-XE-60 columns.

[9/308 Received, 26th February, 1979]

\* Throughout this paper: 1 Torr ≈ (101 325/760) Pa.

#### REFERENCES

- G. N. Schrauzer, R. J. Windgassen, and J. Kohnle, *Chem. Ber.*, 1965, **98**, 3324.
- L. I. Simándi and É. Budó-Záhonyi, *Proc. XIIIth Internat. Conf. Co-ordination Chem., Krakow-Zakopane*, 1970, vol. I, p. 31.
- L. I. Simándi, Z. Szeverényi, and É. Budó-Záhonyi, *Inorg. Nuclear Chem. Letters*, 1975, **11**, 773.
- L. I. Simándi, Z. Szeverényi, and É. Budó-Záhonyi, *Inorg. Nuclear Chem. Letters*, 1976, **12**, 273.
- Y. Ohgo, S. Takeuchi, and J. Yoshimura, *Bull. Chem. Soc. Japan*, 1971, **44**, 283, 583.
- S. Takeuchi, Y. Ohgo, and J. Yoshimura, *Bull. Chem. Soc. Japan*, 1974, 463.
- M. N. Ricroch and A. Gaudemer, *J. Organometallic Chem.*, 1974, **67**, 119.
- T. Yamaguchi and R. Miyagawa, *Chem. Letters*, 1978, 89; T. Yamaguchi and T. Tsumura, *ibid.*, 1973, 409.
- A. Rockenbauer, É. Budó-Záhonyi, and L. I. Simándi, *J. Co-ordination Chem.*, 1972, **2**, 53; 'Stability Constants of Metal-Ion Complexes,' *Special Publ.*, The Chemical Society, London, 1971, no. 25, pp. 341, 360.
- A. E. Martell and M. M. Taqui Khan, 'Homogeneous Catalysis by Metal Complexes,' Academic Press, New York and London, 1974, vol. 1, p. 36.
- L. I. Simándi and F. Nagy, *Acta Chim. Acad. Sci. Hung.*, 1965, **46**, 101, 137.
- T.-H. Chao and J. H. Espenson, *J. Amer. Chem. Soc.*, 1978, **100**, 129.
- Z. Szeverényi, É. Budó-Záhonyi, and L. I. Simándi, *Proc. XVIIth Internat. Conf. Co-ordination Chem., Hamburg, 6–10th September*, 1976, p. 169.
- A. Rockenbauer, É. Budó-Záhonyi, and L. I. Simándi, *J.C.S. Dalton*, 1975, 1729.
- L. I. Simándi and É. Budó-Záhonyi, *Proc. XVIth Internat. Conf. Co-ordination Chem., Dublin, 19–24th August, 1974*, paper 436.
- B. R. James, 'Homogeneous Hydrogenation,' Wiley–Interscience, London, New York, Toronto, 1973.
- H. Gnichtel, *Chem. Ber.*, 1965, **98**, 567.